Cancer Letters 448 (2019) 117–127

Contents lists available at ScienceDirect

Cancer Letters

journal homepage: www.elsevier.com/locate/canlet

Original Articles

Hypoxia induces actin cytoskeleton remodeling by regulating the binding of CAPZA1 to F-actin via PIP2 to drive EMT in hepatocellular carcinoma

Deng Huang[a], Li Cao[a], Le Xiao[a,b], Ju-xian Song[a,c], Yu-jun Zhang[a], Ping Zheng[a], Shu-guo Zheng[a,*]

[a] Institute of Hepatobiliary Surgery, Southwest Hospital, Third Military Medical University (Army Medical University), Chongqing, 400038, China
[b] General Surgery Center, Chengdu Military General Hospital, Chengdu, Sichuan Province, 610083, China
[c] Hepatobiliary Surgery, Libration Army No. 925 Hospital, Guiyang City, Guizhou Province, 550009, China

ARTICLE INFO

Keywords:
Hypoxia-inducible factor-1α (HIF-1α)
RhoA
ROCK1
Invasion
Migration

ABSTRACT

Studies have shown that hypoxia can induce cytoskeletal injury and remodeling through the activation of the RhoA/ROCK signaling pathway by hypoxia-inducible factor-1α (HIF-1α). Our previous study confirmed that CAPZA1 can modulate EMT by regulating actin cytoskeleton remodeling. However, the relationship between HIF-1α and CAPZA1 has not been illustrated. Therefore, this study aimed to investigate the mechanism by which hypoxia induces the remodeling of the actin cytoskeleton by regulating CAPZA1 in hepatocellular carcinoma (HCC) cells. In the present study, we showed that the low expression of CAPZA1 promotes HCC cell invasion and migration in vitro and in vivo by regulating actin cytoskeleton remodeling to drive EMT. Furthermore, we found that the combination of PIP2 and CAPZA1 enables CAPZA1 to be released from the barbed end of F-actin, which in turn drives the remodeling of the actin cytoskeleton. Finally, we confirmed that hypoxia increases PIP2 levels and its binding to CAPZA1 in HCC cells via the HIF-1α/RhoA/ROCK1 pathway. Thus, CAPZA1 and PIP2 could be therapeutic targets to inhibit the invasion and migration promoted by hypoxia in HCC cells.

1. Introduction

Among all malignant tumors, hepatocellular carcinoma (HCC) is characterized by high invasion and metastasis, ranking fifth in incidence and second in mortality [1]. Due to the large number of hepatitis B patients, approximately half of HCC patients are in China. At present, surgical resection is the main treatment for HCC, but the recurrence and metastasis rate is still as high as 70% within 5 years after surgery [2]. Studies have shown that high invasiveness is an important cause of the postoperative recurrence and metastasis of HCC [3]. The epithelial-mesenchymal transition (EMT) is one of the important mechanisms of HCC cell invasion [4]. EMT refers to the biological process of the transformation of epithelial cells into mesenchymal cells under specific microenvironment conditions. Under EMT, the phenotype of HCC cells is transformed, and eventually, these cells acquire the ability of invasion and migration [5,6]. Studies have shown that the essence of EMT is the initiation of actin cytoskeleton remodeling [7,8]. Cytoskeletal remodeling was previously thought to be a result of EMT, but recent studies have found that cytoskeletal remodeling can initiate EMT as an upstream event [9]. The regulation of cytoskeletal remodeling in EMT has become a new insight for preventing HCC from invasion and migration [9–11].

Hypoxia is a common phenomenon in solid tumors that not only kills some tumor cells but also changes the metabolism, gene expression and postexpression modification of another tumor cells [12]. Tumor cells can undergo a series of adaptive changes in the hypoxic environment to promote their proliferation, migration, invasion and drug resistance [13–15]. The liver has a rich blood supply due to the influx of double blood from the portal vein and hepatic artery. Therefore, hypoxia is more prominent during the growth of HCC [16]. The cytoskeleton is highly sensitive to hypoxia. Studies have reported that hypoxia can induce cytoskeletal injury and remodeling through the activation of the RhoA/ROCK signaling pathway by hypoxia-inducible factor-1α (HIF-1α) [17,18]. Since the essence of EMT is the remodeling of the cytoskeleton, hypoxia can directly induce EMT through the RhoA/ROCK pathway, but the specific mechanism remains unclear.

The cytoskeleton is an intricate network of protein filaments throughout the cytoplasm, which is the basis for maintaining cell morphology [19]. Actin filament (F-actin) is an important component of the cytoskeleton and the dynamic remodeling of these filaments provides the impetus for cell invasion and migration [20]. Capping actin protein of muscle Z-line (CapZ) is an actin binding protein that can bind to the barbed end of F-actin. CapZ is a heterodimeric protein comprising α and β subunits [21]. Capping actin protein of muscle Z-

* Corresponding author.
E-mail address: shuguozh@163.com (S.-g. Zheng).

https://doi.org/10.1016/j.canlet.2019.01.042
Received 17 October 2018; Received in revised form 25 January 2019; Accepted 29 January 2019

line alpha subunit 1 (CAPZA1) is the α1 subunit of CapZ. In our previous study, we have confirmed that CAPZA1 promoted EMT in HCC cells by regulating the remodeling of F-actin [11]. However, how the combination of CAPZA1 and F-actin is regulated in tumor cells remains unclear.

Phosphatidylinositol (4,5)bisphosphate (PIP2) is a kind of phospholipid. Although its content is less than 1%, its functions are very complicated [22]. Studies have found that PIP2, as an integrator of signal transduction on the plasma membrane, can regulate biological processes, such as actin cytoskeleton remodeling, which is necessary for cell migration [23]. The mechanism of PIP2 on actin cytoskeleton remodeling has not been elucidated during HCC progression. In the present study, we demonstrate that PIP2 is a negative regulator of CAPZA1 binding to F-actin. Hypoxia can increase the level of PIP2 in tumor cells by activating the HIF-1α/RhoA/ROCK pathway and thus initiate the remodeling of the actin cytoskeleton to drive EMT. Therefore, regulating the level of PIP2 could be a new target for the treatment of HCC cell invasion and migration.

2. Materials and methods

2.1. Cell culture and hypoxia treatment

Human HCC cell lines SMMC-7721 and MHCCLM3 (obtained from the cell bank in our laboratory) were cultured in DMEM (HyClone, USA) containing 10% fetal bovine serum (ZETA life, USA) at 37 °C in a 5% CO_2 humidified incubator. For hypoxia treatment, the cells were cultured in DMEM containing 10% FBS and 400 μM Cobalt(II) chloride hexahydrate ($CoCl_2.6H_2O$) (Sigma-Aldrich, USA) at 37 °C in a 20% O_2 humidified incubator or in DMEM containing 10% FBS at 37 °C in a 1% O_2 humidified incubator for 24 h.

2.2. Reagents and inhibitors

PIP2 reagent (500 ng/L), purchased from SANTA CRUZ (USA), was used to treat the HCC cell lines for 12 h. Neomycin (Sigma-Aldrich, USA) has a high affinity for PIP2 and can isolate PIP2 in cells. The HCC cells were treated with neomycin (500 μM) for 12 h. YC-1 (50 μM) (Sigma-Aldrich, USA), a HIF-1α inhibitor, was used to abolish the accumulation of HIF-1α. C3 transferase protein (0.25 μg/ml) (Cytoskeleton, USA), an inhibitor of RhoA, was used to inhibit the activation of RhoA. Y-27632 (10 μM) (MedChem Express, USA), an inhibitor of ROCK, was used to inhibit the ROCK1 activation.

2.3. Lentiviral infection

CAPZA1 overexpression and interference lentiviruses (LV8-CAPZA1 and LV10-CAPZA1) were constructed by GenePharma Company in Shanghai, China. SMMC-7721 and MHCCLM3 cells were seeded onto 6-well plates, and lentiviral infection was carried out when the cell fusion rate reached 50–70%. For infection, 1 ml of fresh culture medium was replaced, and 10 μl of lentivirus (1×10^9 TU/ml) was added to each well. After 48–72 h, the infection rate was observed using a fluorescence microscope, and CAPZA1 expression levels were detected by western blotting.

2.4. Matrigel invasion assay

Before invasion assays, the transwell chambers (8 μm, 24-well format) (Millipore, USA) were coated with 30 μl of Basement Membrane Matrigel (diluted 1:6 in DMEM; Corning Life Science, USA) for 5 h in a 37 °C incubator. Then, 200 μl of serum-free DMEM containing 6×10^4 cells and 800 μl of DMEM containing 10% FBS were added to the upper and lower wells of the chamber, respectively. Following 36 h of incubation, the chambers were fixed with 4% paraformaldehyde for 30 min, stained with crystal violet (Beyotime, China) for 15 min, and washed with PBS until the residual crystal violet was washed clear. The Matrigel and cells on the upper chamber were gently removed with a cotton swab. The number of invading cells was photographed and counted in three randomly selected × 200 fields under a microscope.

2.5. Wound healing assay

HCC cells were seeded onto the 6-well plates and incubated at 37 °C until the cell fusion degree reached 100%. Wounds were created with a 10 μl pipette tip by scratching straight lines on the cell surface. After washing with PBS three times, the cells were incubated in a cell incubator with serum-free DMEM. Cell migration across the wound lines was monitored at 24 h after scratching.

2.6. Xenograft models

After anesthetizing with 1% sodium pentobarbital (100 ml/kg; Sigma-Aldrich, USA) by intraperitoneal injection, a median abdominal incision of 1 cm was made under the xiphoid of nude mice. After exposing the livers of nude mice, a total of 1×10^5 HCC cells (stable sh-CAPZA1-expressing SMMC-7721 cells, CAPZA1-overexpressing MHCCLM3 cells and corresponding control cells) (50 μl of cell suspension mixed with 30 μl of Matrigel) were injected under the liver capsule. After 6 weeks, a 7.0 T small animal MRI (Bruker Biospec, Germany) was used to scan the mice to observe metastasis of the tumor. After the execution of nude mice, the liver was removed and sliced into paraffin sections. Finally, the sections were stained with hematoxylin and eosin (HE). The animal research was approved by The Institutional Animal Use and Care Committee and complied with the Animal Research Ethics Committee of the Third Military Medical University (Army Medical University).

2.7. Western blot analysis

HCC cells were lysed with RIPA (Beyotime, China) supplemented with protease inhibitors and/or phosphatase inhibitors (Beyotime, China) on ice for 20 min. The lysate was centrifuged for 10 min at 14 000 g at 4 °C. The supernatant is the total protein solution. The concentration of the supernatant was measured, mixed with loading buffer and then boiled for 5 min. The proteins were separated by 10% SDS-PAGE and transferred onto PVDF membranes (Millipore, USA). The PVDF membranes were blocked with 5% skim milk for 2 h at room temperature and incubated with antibodies (Table S1) overnight at 4 °C. The membranes were subsequently incubated with a homologous HRP-conjugated secondary antibody at room temperature for 1 h. The proteins were detected using a gel imaging system (Vilber, France) with Clarity Western ECL Substrate (Bio-Rad, USA).

2.8. Quantitative real-time PCR (qRT-PCR)

Total RNA was extracted with the Ultrapure RNA Kit (CWBIO, China). Reverse transcription was performed according to a reverse transcription reagent protocol (Takara, Japan). PCR primers targeting CAPZA1, E-cadherin, N-cadherin, vimentin and GAPDH were used in this study. The qRT-PCR reactions were performed with SYBR Premix Ex *Taq*II (Takara, Japan) according to the manufacturer's protocols.

2.9. Coimmunoprecipitation

Then, 100 μl of protein A or protein G SureBeads reagent (Bio-Rad, USA) was transferred to a 1.5 ml tube after resuspending in solution. The supernatant was discarded after the beads were magnetized with a magnetic separation rack. Following washing three times with PBST, the beads were incubated in a 200 μl final volume of solution containing 3 μg of CAPZA1 antibody (Proteintech, USA) or F-actin antibody

(Abcam) for at least 30 min at room temperature. The supernatant was discarded and the beads were washed with PBST three times. Then, the beads were resuspended in 500 μl of antigen-containing lysate and incubated at 4 °C with rotating overnight. After discarding the supernatant and washing with PBST three times the next morning, the beads were resuspended in 30 μl of SDS-PAGE loading buffer and boiled for 10 min. The residual buffer was collected and detected by western blotting.

2.10. PIP2 bead affinity precipitation

SMMC-7721 cells were lysed and sonicated in 500 μl of wash/bind buffer containing 10 mM HEPES (pH 7.4), 150 mM NaCl, and 0.25% Nonidet P-40. After centrifugation at 10,000 g at 4 °C for 10 min, the supernatant was mixed with 60 μl of PIP2-conjugated agarose beads (Echelon Bioscience, USA) and incubated at 4 °C overnight with rotating. After washing three times with wash/bind buffer, the beads were heated at 100 °C for 10 min in 30 μl of SDS-PAGE loading buffer. The eluted proteins from the PIP2 beads were detected by CAPZA1 antibody (Proteintech, USA) with western blotting.

2.11. Dot blots

Whole cell lysates from HCC cells were extracted under each hypoxic condition. The lysates were spotted onto a nitrocellulose membrane. The nitrocellulose membranes were blocked with 5% skim milk for 2 h at room temperature and incubated with PIP2 (2C11) antibody (1:200, SANTA CRUZ, USA) and GAPDH (1:5,000, ABclonal, USA) at 4 °C overnight. After incubation with a homologous HRP-conjugated secondary antibody at room temperature for 1 h, the membranes were detected using a gel imaging system (Vilber, France) with Clarity Western ECL Substrate (Bio-Rad, USA).

2.12. PIP2 ELISA assay

Whole cell lysates were extracted from HCC cells under hypoxic conditions with RIPA lysis buffer and sonication. The Human Phosphatidylinositol (4,5)bisphosphate (PIP2) Kit was purchased from the Shanghaijining Company (N112976). The standard wells were set according to the manufacturer's instructions, and 50 μl of whole cell lysate was added to the sample wells. Then, 100 μl of homologous HRP-conjugated secondary antibody were added to the standard and sample wells, followed by incubating at 37 °C for 1 h. The supernatant was discarded, and the wells were washed five times with 350 μl of wash buffer. Next, 50 μl of substrates A and B were added into each well and incubated for 15 min at 37 °C without light. The reaction was stopped with 50 μl of stop buffer and detected by a Nano drop spectrophotometer (Thermo, USA) at 450 nm.

2.13. Active RhoA pull-down assay

HCC cells were cultured in medium (with 400 μM $CoCl_2$) at 37 °C for 24 h after the addition of C3 or PBS. The cells were lysed on ice after rinsed twice with ice-cold PBS. And then, the lysate protein concentrations were determined using BCA protein assay. According to the instructions of Active Rho Detection Kit (Cell Signaling Technology, USA), GST-Rhotekin-RBD fusion protein was used to bind the activated Rho protein. The levels of the activated form of RhoA, RhoA-GTP, were determined by western boltting using a RhoA Rabbit antibody (Proteintech, USA).

2.14. Immunofluorescence

HCC cells were briefly seeded on clean glass cover slips. After washing with PBS, the cells on the cover slips were fixed with 4% paraformaldehyde for 20 min. The cover slips were rinsed 3 times with PBS for 3 min each. The cells were permeabilized with 0.2% Triton X-100 in PBS for 5 min and incubated with a blocking solution of 5% goat serum in PBS for 30 min. The blocking solution was aspirated, and the cells were incubated with CAPZA1 antibody (1:100, Proteintech, USA), or PIP2 (2C11) antibody (1:50, SANTA CRUZ, USA) overnight at 4 °C. The cover slips were washed with PBS 3 times for 3 min each. The cover slips were incubated with Alexa Fluor 488-conjugated and/or Alexa Fluor 594-conjugated secondary antibodies (1:200, Proteintech, USA) for 1 h in a moist, dark environment. After washing with PBS, phalloidin labeled with rhodamine (1:200, Solarbio, China) was used to label the F-actin for 30 min at room temperature. Then, 10 μl of antifade mounting medium containing DAPI (VECTASHIELD, USA) was added to the cover slips for nuclear staining.

2.15. Extraction of cytoplasmic and cytoskeletal proteins

The cytoplasmic and cytoskeletal proteins were extracted with the Subcellular Structure Protein Extraction Kit (Sangon, China) according to the manufacturer's instructions. A standard number of cells (2×10^6) was used in each sample. Each sample was mixed with 500 μl of cold Extraction buffer 1 supplemented with 5 μl of protease inhibitor and shaken on ice for 10 min. The supernatant was collected and saved after centrifugation at 3000 rpm for 8 min at 4 °C. The cytoplasmic proteins were present in the supernatant. The residual precipitation was resuspended with 200 μl of Extraction buffer 4. Then, the sample was centrifuged at 12000 g for 15 min at 4 °C. The residual precipitation was dissolved with 200 μl of 1 × loading buffer after washing twice with −20 °C with 90% acetone. The cytoskeletal proteins were dissolved in loading buffer. The protein levels were detected by western blotting.

2.16. Cases and follow-up

In this study, we analyzed 154 HCC patients who received pathological liver resection at Southwest Hospital between January 2010 and December 2012. The clinicopathologic data (gender, age, tumor size, TNM stage, HCC differentiation, lymph node metastasis, vascular invasion and other information) for the patient were collected by inquiring patient records and pathological examination. The patients were followed up until 5 years after surgery, and tumor recurrence and patient death were recorded. All subjects signed an informed consent form. The study was approved by the institutional research ethics committee of Southwest Hospital.

2.17. Immunohistochemical staining

The patient pathological tissues were made into a tissue array including 60 pairs of cancer and paracancer tissues, and 94 cases of HCC tissue. After dewaxing and hydration, the tissue arrays were heated in sodium citrate solution for antigen retrieval. After naturally cooling, the array was incubated in 3% H_2O_2 for 10 min and blocked in 10% goat serum at room temperature for 1 h. The arrays were incubated with anti-CAPZA1 (1:50, Proteintech, USA), anti−HIF−1α (1:100, Proteintech, USA), anti-E-cadherin (1:100, Abcam, USA), anti-Vimentin (1:100, Proteintech, USA) and anti-PIP2 (2C11) (1:50, SANTA CRUZ, USA) antibodies overnight at 4 °C. An anti-mouse/rabbit immunohistochemical detection kit (ZSGB-Bio, China) was used to detect the Immunohistochemical reaction. Finally, the arrays were dehydrated, stained with hematoxylin and mounted with neutral resin.

2.18. Statistical analysis

Statistical analyses were conducted by SPSS 19.0 (SPSS Inc., USA) for Windows and Prism 6 (GraphPad, USA). Continuous variables were expressed as the means ± standard deviation and compared using the Independent Sample *t*-test and the Mann-Whitney *U* test. For categorical variables, comparisons were made using chi-square analysis or

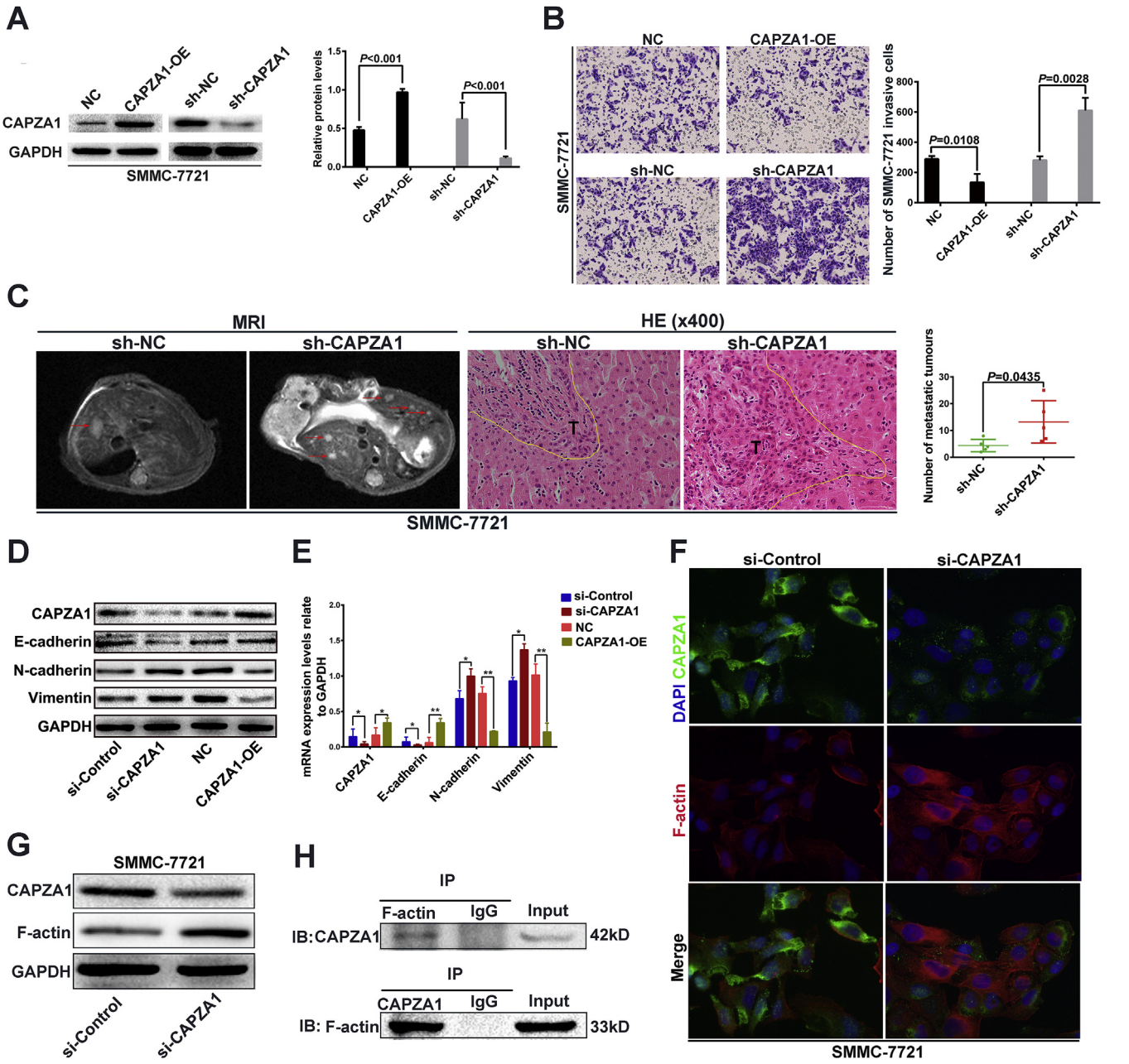

Fig. 1. Downregulation of CAPZA1 expression drives HCC EMT by regulating actin cytoskeleton remodeling. (A) CAPZA1 overexpression and interference were performed in SMMC-7721 cells. (B) The upregulation of CAPZA1 decreased the invasion of SMMC-7721 cells, and the downregulation of CAPZA1 enhanced the invasion of SMMC-7721 cells. (C) Small animal MRI scan. The intrahepatic tumor metastases (Indicated by red arrowheads in MRI pictures and marked as "T" in HE pictures) of nude mice grown with sh-CAPZA1-expressing SMMC-7721 cells were significantly higher than those in the control mice. (D, E) Western blotting and qRT-PCR were performed to detect the expression of EMT related markers. The downregulation of CAPZA1 inhibited the expression of the epithelial marker E-cadherin and enhanced the expression of the mesenchymal markers N-cadherin and Vimentin; when the expression of CAPZA1 was upregulated, these results were reversed. (F) Immunofluorescence of CAPZA1 and F-actin on SMMC-7721 cells showed that the level of F-actin in the si-CAPZA1 group was significantly increased. (G) Western blotting showed that the interference of CAPZA1 expression increased the F-actin level. (H) IP confirmed that CAPZA1 could interact with F-actin. $^{*}P < 0.05$, $^{**}P < 0.01$, $^{***}P < 0.001$. (For interpretation of the references to colour in this figure legend, the reader is referred to the Web version of this article.)

Fisher's exact test. All statistical tests were two-way. $P < 0.05$ was considered statistically significant.

3. Results

3.1. Downregulation of CAPZA1 expression drives HCC EMT by regulating actin cytoskeleton remodeling

To observe the role of CAPZA1 on the invasion and migration of HCC cells, we performed Matrigel invasion and wound healing assays in vitro. First, we detected the expression of CAPZA1 in MHCCLM3, Huh7, MHCC97h, MHCC97L, SMMC-7721 and HepG2 cell lines using western blotting. The expression of CAPZA1 was lowest in the HCCLM3 cell line and highest in the SMMC-7721 cell line (Fig. S1A). Then, CAPZA1 overexpression and interference were performed in MHCCLM3 and SMMC-7721 cells (Fig. 1A, Fig. S1C). The upregulation of CAPZA1 expression decreased the invasion and migration of SMMC-7721 cells. In contrast, the downregulation of CAPZA1 expression enhanced the invasion and migration of SMMC-7721 cells (Fig. 1B, Fig. S1B). These phenomena were also observed in MHCCLM3 cells (Figs. S1D and E).

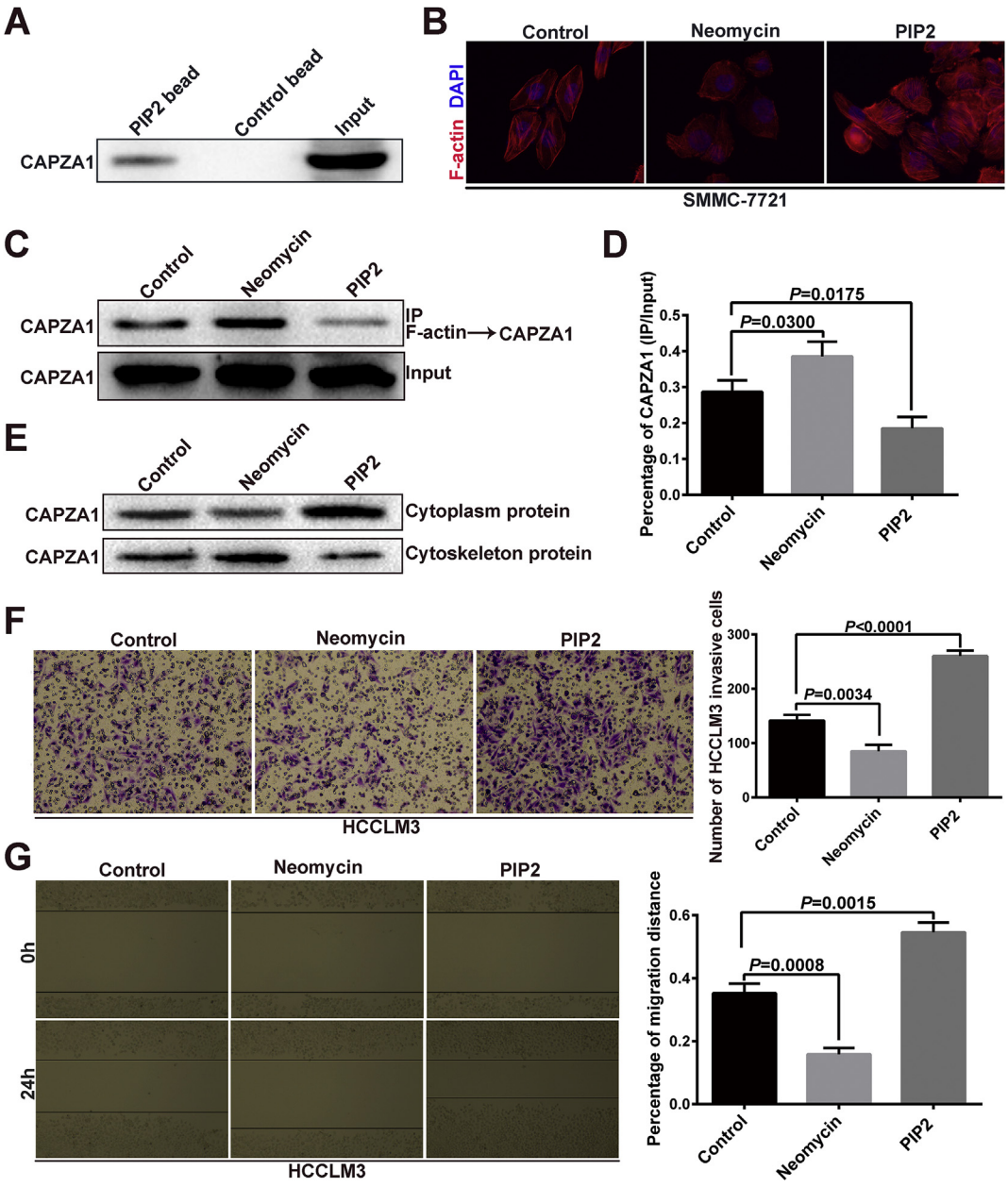

Fig. 2. PIP2 regulates the binding of CAPZA1 to the barbed end of F-actin. (A) CAPZA1 was pulled down by the beads coated with PIP2. (B) The level and structure of F-actin and the cell morphology were changed after treatment with neomycin and PIP2. (C, D) The binding level of CAPZA1 to F-actin was increased after treatment with neomycin and was decreased after treatment with PIP2. (E) The distribution of CAPZA1 in the subcellular structure. CAPZA1 was more bound to the cytoskeleton and less distributed in the cytoplasm after cells were treated with neomycin; CAPZA1 was less bound to the cytoskeletonand and more distributed in the cytoplasm after treatment with PIP2. (F, G) The capacity of invasion and migration was inhibited after treatment with neomycin, and was enhanced after treatment with PIP2.

The in vitro experiments verified that CAPZA1 can inhibit the invasion and migration of SMMC-7721 and HCCLM3 cells. Furthermore, we observed that in the animal experiment the intrahepatic tumor metastases of nude mice grown with sh-CAPZA1-expressing SMMC-7721 cells were significantly higher than those in the control group mice (Fig. 1C) and the intrahepatic tumor metastases of nude mice grown with CAPZA1-overexpressing MHCCLM3 cells were significantly less than those in the control group mice (Fig. S1F).

EMT is one of the important mechanisms by which HCC cells disseminate from the primary lesion. E-cadherin is a major component of epithelial adherens junctions which mediate intercellular adhesion along with tight junctions. N-caherin belongs to classical cadherins family and forms hemophilic cell-cell adhesion junctions [7]. Vimentin, a intermediate filament protein, participates in numerous cellular processes including cell adhesion, migration and invasion [10]. The loss of epithelial E-cadherin and gain of mesenchymal N-cadherin and vimentin expression is a major hallmark of EMT. A recent study reported that actin cytoskeleton remodeling drives EMT for hepatoma invasion and metastasis in mice [9]. CAPZA1 is an important actin filament binding protein that participates in the regulation of actin cytoskeleton remodeling. Therefore, in the present study, we investigated the role of CAPZA1 as a regulator of EMT by modulating actin cytoskeleton remodeling in HCC cells. The results of the western blot analysis and qRT-PCR showed that when the expression of CAPZA1 was downregulated, the epithelial marker E-cadherin was downregulated and the mesenchymal markers N-cadherin and Vimentin were upregulated; when

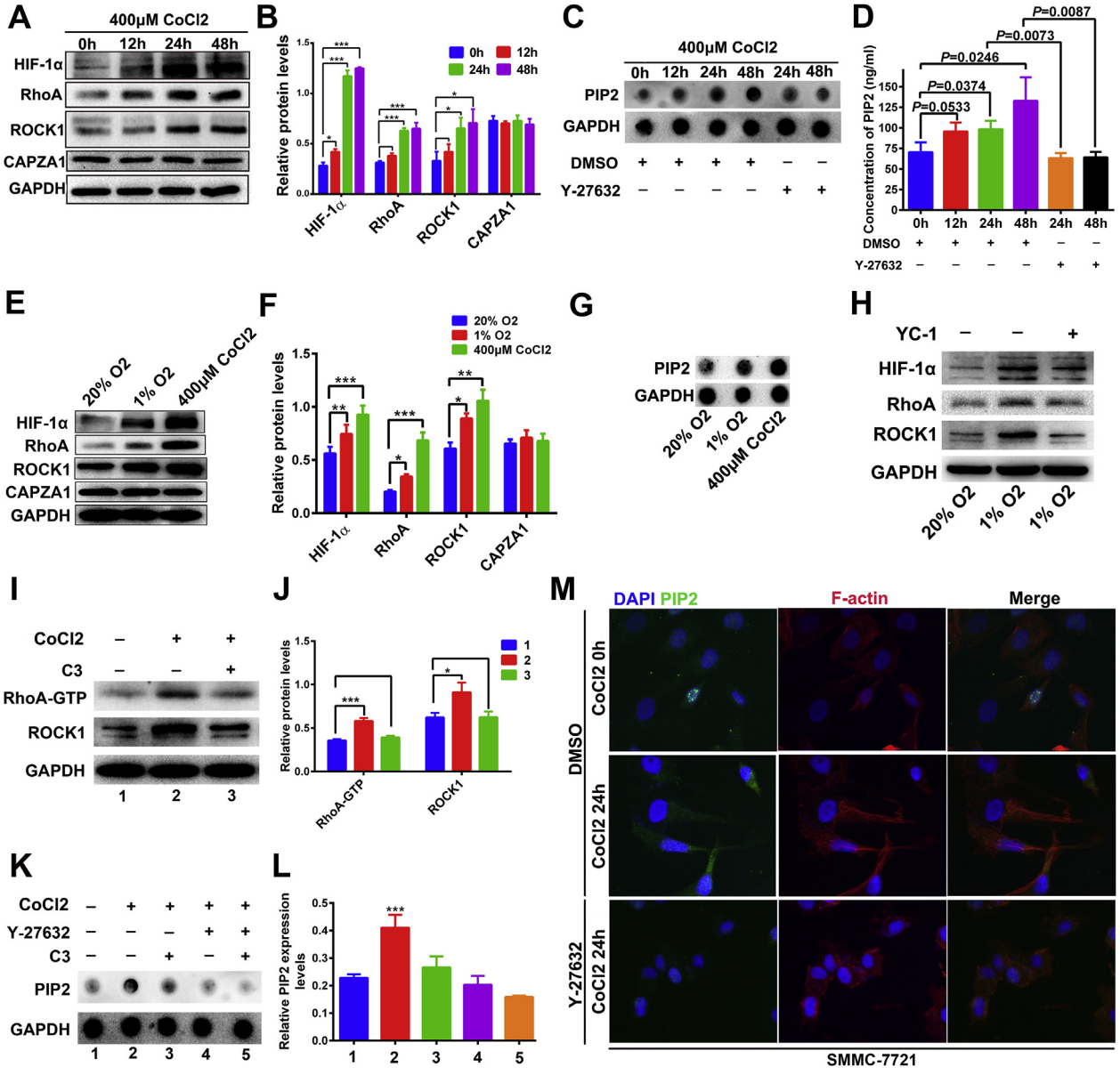

Fig. 3. Hypoxia increases the PIP2 level by activating the HIF-1α/RhoA/ROCK1 signaling pathway. (A, B) The expression of HIF-1α, RhoA and ROCK1 increased with $CoCl_2$ treatment, especially with $CoCl_2$ treatment for 24 h, but the expression of CAPZA1 did not change with the treatment. (C, D) Dot blot analysis and ELSA showed that PIP2 levels gradually increased with the time of $CoCl_2$ treatment, and the increase in PIP2 levels was inhibited by Y-27632. (E, F) The treatment of $CoCl_2$ for 24 h had the same effect on HCC cells as 1% O_2 induction for 24 h. Both $CoCl_2$ treatment and hypoxia induction increased the expression of HIF-1α, RhoA and ROCK1, but did not affect the expression of CAPZA1. (G) Both $CoCl_2$ treatment and 1% O_2 induction for 24 h had the same role to increase the PIP2 level. (H) The expression of HIF-1α, RhoA and ROCK1 was increased after hypoxia treatment. However, the addition of YC-1, an inhibitor of HIF-1α, inhibited the expression of HIF-1α, RhoA and ROCK1 induced by hypoxia. (I, J) Active RhoA pull-down and western blotting assays confirmed that hypoxia treatment (treated with 400 μM $CoCl_2$ for 24 h) increased the levels of RhoA-GTP and ROCK1, while the RhoA inhibitor C3 transferase inhibited these trends. (K, L) The level of PIP2 was significantly increased after hypoxia treatment (treated with 400 μM $CoCl_2$ for 24 h). The addition of C3 transferase and/or Y-27632 blocked the increase of PIP2 level caused $CoCl_2$ treatment. (M) The level of PIP2 was significantly increased, and the enrichment of F-actin was in the region with more PIP2 distribution with hypoxia treatment (treated with 400 μM $CoCl_2$ for 24 h). The morphology of the cells with hypoxia treatment changed into a long fusiform shape. All of these changes were inhibited by Y-27632. $^*P < 0.05$, $^{**}P < 0.01$, $^{***}P < 0.001$.

the expression of CAPZA1 was upregulated, the results were reversed (Fig. 1D and E). Subsequently, the regulation of CAPZA1 in actin cytoskeleton remodeling was observed by immunofluorescence. Compared with the control group, the level of F-actin in si-CAPZA1 group was significantly increased (Fig. 1F). This result was also confirmed by western blotting (Fig. 1G). However, when the expression of CAPZA1 was upregulated in MHCCLM3 cells, the level of F-actin was decreased (Fig. S2A). In addition, in the si-CAPZA1 group, the HCC cells presented an obvious long fusiform shape, and the F-actin was distributed along the long axis of the cells (Fig. 1F, Fig. S1G). Finally, the results of the coimmunoprecipitation experiment showed that CAPZA1 can interact with F-actin (Fig. 1H).

3.2. PIP2 regulates the binding of CAPZA1 to the barbed end of F-actin

PIP2 regulates many actin regulatory proteins. The change of the PIP2 level in cells has a profound effect on the actin cytoskeleton [24]. Therefore, to investigate whether PIP2 could regulate CAPZA1 directly, we performed a PIP2 bead affinity precipitation assay. The results showed that beads coated with PIP2 pulled down CAPZA1 (Fig. 2A).

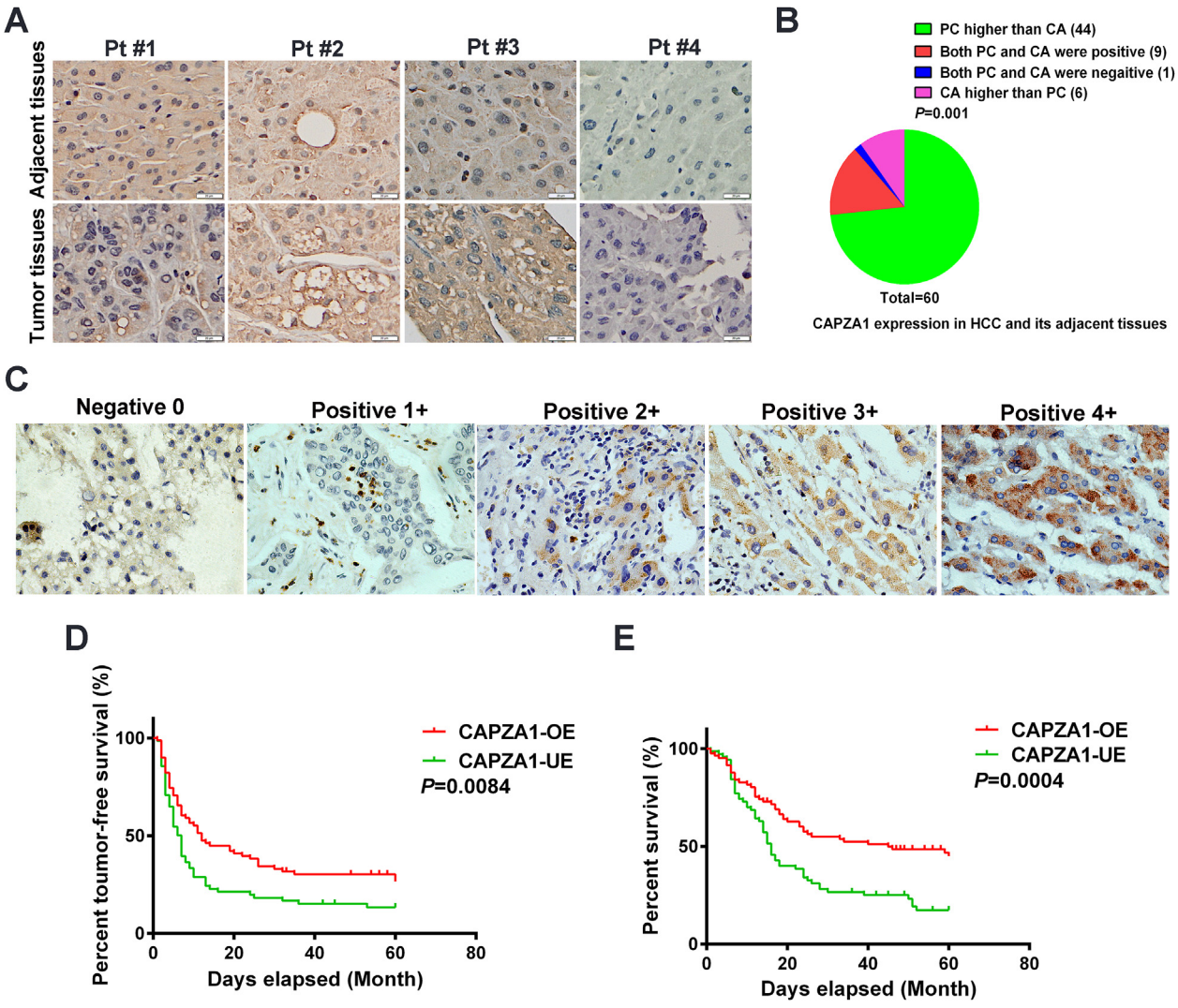

Fig. 4. The poor expression of CAPZA1 is associated with the malignancy of HCC. (A) Representative images of the samples in which CAPZA1 expression was higher in PC than in CA (Pt #1), CAPZA1 expression were both positive in PC and CA (Pt #2), CAPZA1 expression was higher in CA than in PC (Pt #3) and CAPZA1 expression were both negative in PC and CA (Pt #4). (B) Among the 60 paired tissues, CAPZA1 expression was higher in PC than in CA in 44 cases. (C) Representative images of the expression of CAPZA1 in HCC tissues scored 0, 1+, 2+, 3 + and 4+. (D, E) The tumor-free survival time and survival time of HCC patients in the CAPZA1 underexpression group were significantly lower than those in the overexpression group at 5 years after surgery.

The experiment confirmed that PIP2 can combine with CAPZA1. Subsequently, a series of experiments was performed to investigate the role of the binding on the actin cytoskeleton remodeling. The immunofluorescence results showed that the level of F-actin was decreased, the structure was scattered and the morphology of the cells became round after treatment with the PIP2 inhibitor neomycin in HCC cells. In contrast, the F-actin level in cells treated with PIP2 was increased significantly (Fig. 2B). In addition, the increase in the F-actin level induced by CAPZA1 depletion was inhibited when treated with the PIP2 inhibitor neomycin. When treated with PIP2, the F-actin level was increased, similar to the result of CAPZA1 interference (Fig. S2B). Then, we investigated whether the binding of PIP2 to CAPZA1 regulates the binding of CAPZA1 to the barbed end of F-actin. In the same number of HCC cells, we observed changes in the binding level of F-actin and CAPZA1 using IP experiments. The expression of CAPZA1 in HCC cells did not change after treatment with neomycin or PIP2, but the binding amounts of F-actin and CAPZA1 were increased or decreased, respectively (Fig. 2C and D). Additionally, we observed the subcellular localization of CAPZA1 when treated with neomycin or PIP2. CAPZA1 was more bound to the cytoskeleton and less distributed in the cytoplasm after the cells were treated with neomycin, while CAPZA1 was less bound to the cytoskeleton and more distributed in the cytoplasm after treatment with PIP2 (Fig. 2E). Finally, we also detected the changes in the invasion and migration capacity of HCCLM3 cells. The capacity of invasion and migration was inhibited after treatment with neomycin, and was enhanced after treatment with PIP2 (Fig. 2F and G).

3.3. Hypoxia increases the PIP2 level in HCC cells by activating the HIF-1α/RhoA/ROCK1 signaling pathway

Hypoxia is a common phenomenon in solid tumors, especially in HCC [25]. Persistent hypoxia in the HCC microenvironment can change the metabolism and gene expression of tumor cells and accelerate the aggressiveness of HCC cells [26,27]. Therefore, we investigated the relationship between hypoxia and PIP2. First, we used the $CoCl_2$ treatment as a hypoxia mimetic and found that the $CoCl_2$ treatment can increase the expression levels of HIF-1α, RhoA and ROCK1 especially with the treatment for 24 h. However, the expression of CAPZA1 did not change with the treatment (Fig. 3A and B). Then, PIP2 levels were measured by dot blot analysis. The results showed that PIP2 levels gradually increased with the time of $CoCl_2$ treatment, especially after 24 h. This result was consistent with the change of the expression of

Table 1
Comparison of the clinicopathological features and Patient prognosis in the CAPZA1 underexpression and overexpression.

	Levels of CAPZA1 expression		*P*-value
	Underexpression 0,1 + (n = 71)	Overexpression 2+,3+,4+ (n = 83)	
Mean tumor size(cm)	7.8 ± 3.3	6.8 ± 3.6	0.062
TNM stage			0.002
Stage I	9 (12.7%)	23 (27.7%)	
Stage II	7 (9.9%)	12 (14.5%)	
Stage III	33 (46.5%)	41 (49.4%)	
Stage IV	22 (31.0%)	7 (8.4%)	
HCC differentiation			0.001
WD	2 (2.8%)	8 (9.6%)	
MD	48 (67.6%)	69 (83.1%)	
PD	21 (29.6%)	6 (7.2%)	
Lymph node metastasis (Yes/No)	9/62 (12.7%)	3/80 (3.6%)	0.037
Vascular invasion(Yes/No)	32/39 (45.1%)	24/59 (28.95)	0.038
Postoperative recurrence (Yes/No)	58/13 (81.7%)	56/27 (67.5%)	0.045
Cancer related death (Yes/No)	56/15 (78.9%)	43/40 (51.8%)	0.000

HCC, hepatocellular carcinoma. WD, well differentiated. MD, moderately differentiated. PD, poorly differentiated. CAPZA1, Capping actin protein of muscle Z-line alpha subunit 1.

HIF-1α, RhoA and ROCK1 (Fig. 3C). The changes in PIP2 with the $CoCl_2$ treatment were also confirmed by PIP2 ELSA (Fig. 3D). Interestingly, with the addition of Y-27632, a ROCK1 inhibitor, PIP2 levels no longer changed with $CoCl_2$ treatment, even when treated with $CoCl_2$ for 24 or 48 h (Fig. 3C and D).

Additionally, to detect whether the $CoCl_2$ treatment had the same effect as hypoxia, the cells were cultured in a low O_2 incubator. The results showed that the SMMC-7721 cells treated with 400 μM $CoCl_2$ for 24 h were similar to those cultured at 37 °C in a 1% O_2 incubator for 24 h in the expression of HIF-1α, RhoA, ROCK1, CAPZA1 and PIP2 (Fig. 3 E, F and G). Therefore, we believed that the treatment of 400 μM $CoCl_2$ for 24 h was an effective hypoxia mimetic.

Then, we investigated the effects of HIF-1α, RhoA, ROCK1 and PIP2 on the actin cytoskeleton remodeling. The expression of HIF-1α, RhoA and ROCK1 was increased after hypoxia treatment. However, the addition of YC-1, a HIF-1α inhibitor, inhibited the expression of HIF-1α, RhoA and ROCK1 induced by hypoxia (Fig. 3H). The active RhoA pull-down assay showed that the level of RhoA-GTP was increased in HCC cells after $CoCl_2$ treatment. However, the increased level of RhoA-GTP induced by $CoCl_2$ treatment was inhibited by the C3 transferase. Interestingly, the increased ROCK1 level was also inhibited by the RhoA inhibitor C3 transferase (Fig. 3I and J). In order to verify whether RhoA and ROCK1 were involved in the regulation process of hypoxic-induced PIP2 level increase, the RhoA inhibitor C3 transferase or the ROCK1 inhibitor Y-27632 was added into the culture medium during $CoCl_2$ treatment of HCC cells. We found that with the addition of C3 and/or Y-27632, the increased level of PIP2 induced by $CoCl_2$ treatment was abolished (Fig. 3K and L). Finally, we observed the role of PIP2 in the actin cytoskeleton remodeling under hypoxic environments. We found that after 24 h of $CoCl_2$ treatment, the level of PIP2 was significantly increased in HCC cells, and the enrichment of F-actin was in the region with more PIP2 distribution. The morphology of the cells with $CoCl_2$ treatment changed into a long fusiform shape. Howere, all of these changes were inhibited by the ROCK inhibitor Y-27632 (Fig. 3M). Therefore, we believed that the HIF-1α/RhoA/ROCK1 signaling pathway was involved in the regulation of hypoxic-induced PIP2 level increase.

3.4. The poor expression of CAPZA1 is associated with the malignancy of HCC

Of the 154 patients with HCC in the present study, 15 were female and 139 were male. The average age of the patient cohort was 47.8 ± 10.5 years.

CAPZA1 immunohistochemistry was conducted on the tissue array including 60 pairs of carcinoma tissue (CA) and adjacent para-carcinoma tissue (PC) and 94 cases of HCC tissue. Among the 60 paired tissues, CAPZA1 expression was higher in PC than in CA in 44 cases ($P = 0.001$) (Fig. 4A and B). According to the percentage of positively stained HCC cells, the expression of CAPZA1 in HCC tissues was scored as follows: 0 (0%), 1+ (1–24%), 2+ (25–49%), 3+ (50–74%), and 4+ (75–100%) (Fig. 4C). The expression scores of 0 and 1 + were defined as the CAPZA1 underexpression group (n = 71), while 2+, 3 + and 4 + were defined as the CAPZA1 overexpression group (n = 83). Then, we analyzed the effect of CAPZA1 expression on HCC pathological characteristics and the prognosis of HCC patients. By TNM staging, there were more cases in TNM stage III-IV in the CAPZA1 underexpression group than in the CAPZA1 overexpression group ($P = 0.002$). By HCC differentiation class, there were 21 cases of poor differentiation in the CAPZA1 underexpression group, which was more than that in the CAPZA1 overexpression group ($P = 0.001$). The rate of lymphoid tissue (12.7% vs 3.6%; $P = 0.037$) and vascular (45.1% vs 28.9%; $P = 0.038$) invasion was significantly higher in the CAPZA1 underexpression group than in the overexpression group. The recurrence rate (81.7% vs 67.5%; $P = 0.045$) and mortality (78.9% vs 51.8%; $P = 0.000$) at 5 years after surgery in the CAPZA1 underexpression group were significantly higher than those in the overexpression group (Table 1). Additionally, the tumor-free survival and survival time at 5 years after surgery of HCC patients in the CAPZA1 underexpression group were significantly lower than those in the overexpression group (Fig. 4D and E).

3.5. The expression of CAPZA1 is negatively correlated with EMT in HCC tissue

Subsequently, immunohistochemistry was used to detect the expression of E-cadherin and Vimentin, markers of EMT, in HCC tissues. Statistically, the expression of CAPZA1 was positively correlated with the E-cadherin expression (Fig. 5A and B) and negatively correlated with the Vimentin expression in HCC tissues (Fig. 5C and D).

T.Nishikawa has reported that immunohistochemistry can be used to stain PIP2 on the paraffin-embedded brain tissue slides of Alzheimer's disease patients with a PIP2 (2C11) antibody [28]. Our preliminary immunohistochemical assay also showed that the PIP2 on paraffin-embeded HCC tissue slides had not been wipe out during the dewax producedure. The binding of PIP2 (2C11) antibody to PIP2 was effectively prevented by pre-incubation with neomycin (Fig. S3). Finally, we performed immunohistochemical staining in HCC tissue continuous sections to clarify the expression relationship between HIF-1α and PIP2 in HCC tissue. The results showed that the expression of HIF-1α and PIP2 in HCC was positively correlated (Fig. 5E and F).

4. Discussion

The invasion and metastasis of cancer are landmark events in which cancer cells escape from the primary lesion and settle in other organs, threatening the life of the patient. The initial steps in the local invasion of cancer cells involve the activation of cytoskeletal remodeling-associated signaling pathways [29,30]. Cell migration is a complex process that requires the remodeling of the cytoskeleton to form a pseudopodium, including filopodia and lamellipodia, at the leading edge [31]. Therefore, it is important to understand the mechanism of the regulation of cytoskeletal remodeling during cancer cell invasion and migration. Hypoxia is a common phenomenon in solid tumors and an

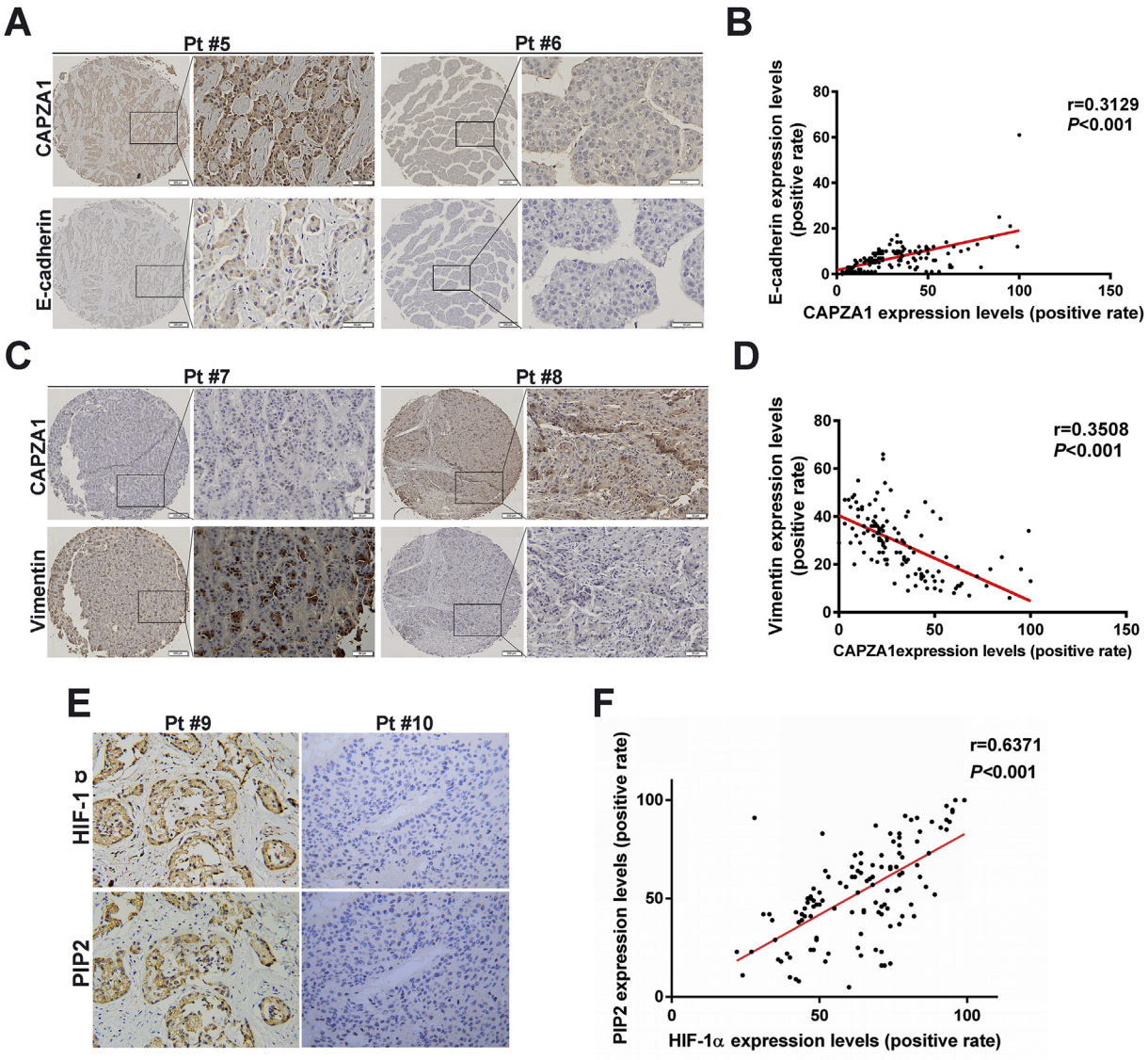

Fig. 5. The expression of CAPZA1 was negatively correlated with EMT in HCC tissues. (A) Representative images of samples in which CAPZA1 and E-cadherin expression were both positive (Pt #5) and negative (Pt #6). (B) CAPZA1 was positively correlated with the expression of E-cadherin in HCC tissues. (C) Representative images of samples in which CAPZA1 expression was low while Vimentin expression was high (Pt #7) and CAPZA1 expression was high while Vimentin expression was low (Pt #8). (D) CAPZA1 was negatively correlated with the expression of Vimentin in HCC tissues. (E) Representative images of HIF-1α and PIP2 expression in HCC tissue continuous sections. (F) The positive expression relationship of HIF-1α and PIP2 was confirmed by immunohistochemical staining in HCC tissue continuous sections.

important stimulant to initiate the invasion and metastasis of cancer cells [32]. In this study, we demonstrated that hypoxia can increase PIP2 levels and its binding to CAPZA1 in HCC cells by activating the RhoA/ROCK1 pathway and thus modulate the remodeling of the actin cytoskeleton. Our findings are consistent with those of other studies reporting that hypoxia can activate signaling pathways that control cytoskeletal dynamics to initiate cancer cell invasion and migration [33,34].

EMT is a crucial mechanism of tumor cell invasion and metastasis. Actin filament is an important component of the cytoskeleton and is deeply involved in the initiation and progression of EMT [9,35]. CAPZA1, an actin binding protein, can bind to the barbed ends of actin filaments, maintaining the stability of the actin cytoskeleton [36]. The role of CAPZA1 in HCC has rarely been reported. In the present study, we manipulated the expression of CAPZA1 in HCC cells. The down-regulation of CAPZA1 expression promoted the invasion and migration of HCC cells in vitro and in vivo, while the upregulation of CAPZA1 inhibited this activity. Additionally, the alteration of CAPZA1 expression changed the degree of EMT and the level of F-actin in HCC cells. Therefore, we reported that CAPZA1, which is abnormally expressed in HCC cells, can regulate the remodeling of the actin cytoskeleton to drive EMT. CAPZA1 is similar to other actin binding proteins [9,37,38].

PIP2 is a kind of phospholipids. Although its level is less than 1%, PIP2 function is very complicated [39]. PIP2 is a key molecule in the G protein-coupled receptor signal transduction pathway. In this signaling pathway, extracellular signaling molecules bind to the G protein-coupled receptor on the cell surface, activate phospholipase C on the plasma membrane, and hydrolyze PIP2 into 1,4, 5-triphosphoinositide (IP3) and diacylglycerol (DG). This signaling system is also known as the “double messenger system” [40]. Recent studies have found that PIP2, as an integrator of signal transduction on the plasma membrane, can regulate biological processes, such as actin filament cytoskeletal remodeling, which is necessary for cell migration [41,42]. In the present study, we found that PIP2 could bind to CAPZA1, which changed the distribution of CAPZA1 in the cytoplasm and cytoskeleton.

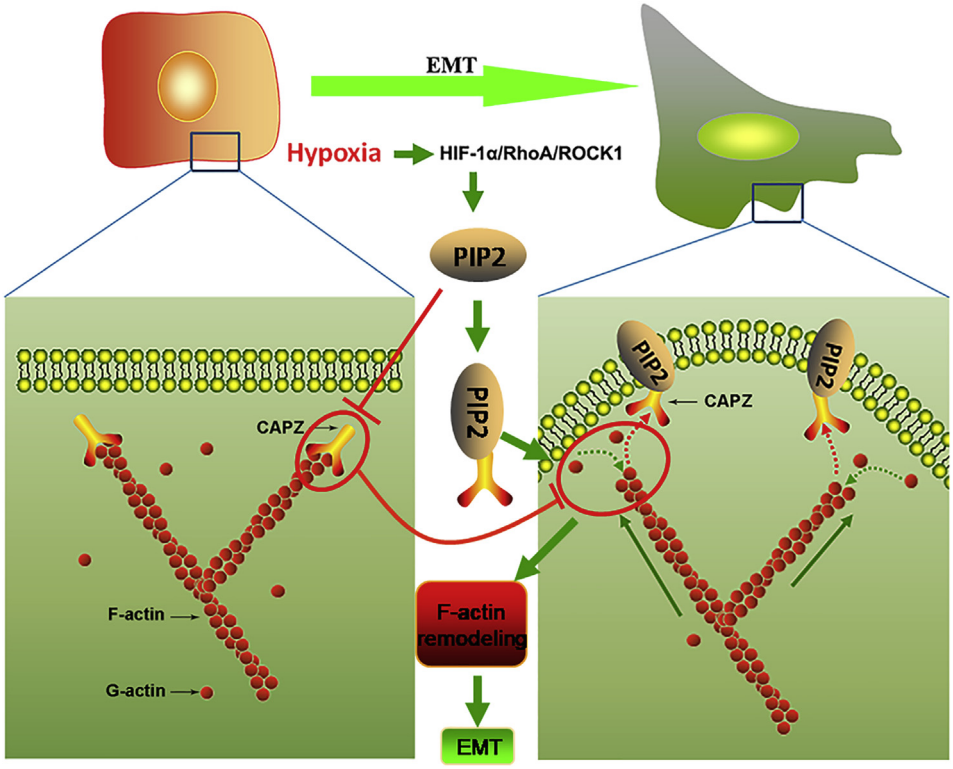

Fig. 6. The mechanism of hypoxia induced EMT in HCC cells. Hypoxia increases PIP2 levels and its binding to CAPZA1 in HCC cell by activating the HIF-1α/RhoA/ROCK1 pathway. Then, the combination of PIP2 and CAPZA1 enables CAPZA1 to be released from the barbed end of F-actin, which in turn drives the remodeling of actin cytoskeleton to promote the EMT of HCC cells.

Moreover, after PIP2 was added to the medium, CAPZA1 was less bound to F-actin, and the level of F-actin was significantly increased. In contrast, CAPZA1 was more bound to F-actin, and the level of F-actin was significantly decreased after the PIP2 inhibitor Y-27632 was added. Therefore, we demonstrated that PIP2 could bind to CAPZA1, which caused CAPZA1 to release from the barbed ends of actin filaments, thus promoting the remodeling of the actin cytoskeleton. Our result is consistent with those of previous studies, which reported that the regulation of CAPZ on the remodeling of the actin cytoskeleton can be regulated by PIP2 in a ventricular myocyte hypertrophy model [43,44].

RhoA/ROCK is an important signaling pathway that regulates the dynamics of the actin cytoskeleton, which can be activated by many stimulators, including mechanical stress and hypoxia, during cell invasion and migration [45,46]. In the present study, the RhoA/ROCK1 signaling pathway was activated under hypoxia by HIF-1α, and the signaling pathway inhibitors, C3 and Y-27632, inhibited the change in hypoxia-induced PIP2 levels in HCC cells. Finally, the consistency of F-actin and PIP2 distribution was disturbed by Y-27632. Our views are in line with those of J. Li, who reported that a possible mechanism for cell hypertrophy was the accumulation of thin filament assembly triggered partially by the increased PIP2 level via the RhoA/ROCK signaling pathway in response to mechanical strain [44].

Finally, we reported that the poor expression of CAPZA1 is associated with the malignancy of HCC. Tumors with the underexpression of CAPZA1 showed malignant behavior, and the patients in the CAPZA1 underexpression group had a poor prognosis. Moreover, the expression of CAPZA1 was negatively correlated with EMT of HCC and the expression of HIF-1α and PIP2 in HCC was positively correlated in HCC tissues.

In conclusion, our study shows that the low expression of CAPZA1 promotes HCC cell invasion and migration in vitro and in vivo. We demonstrate that the combination of PIP2 and CAPZA1 enables CAPZA1 to be released from the barbed end of F-actin, which in turn drives the remodeling of the actin cytoskeleton to promote the EMT of HCC cells. Furthermore, hypoxia increases PIP2 levels and its binding to CAPZA1 in HCC cells via the HIF-1α/RhoA/ROCK1 pathway (Fig. 6). Thus, CAPZA1 could be a therapeutic target to inhibit the invasion and migration driven by hypoxia in HCC cells and a potential clinical biomarker to predict the outcome of HCC patients. Regulating the level of PIP2 in HCC cells may be a new method to inhibit HCC invasion and metastasis.

Formatting of funding sources

This project was supported by the National Natural Science Foundation of China [81670597].

Conflicts of interest

The authors declare that no conflicts of interest exist.

Acknowledgments

We thank the Institute of Hepatobiliary Surgery, Southwest Hospital for providing human HCC tissues and the Department of Clinical Microbiology and Immunology, Third Military Medical University (Army Medical University) for providing the low O_2 humidified incubator. We also thank Mr. Peng Jiang (Institute of Hepatobiliary Surgery, Southwest Hospital, Third Military Medical University (Army Medical University), Chongqing, China) for technical assistance in cell cultureand and Dr. Kaiyuan Zhang (Institute of Neurosurgery, Southwest Hospital, Third Military Medical University (Army Medical University), Chongqing, China) for providing the Active Rho Detection Kit.

Abbreviations

CapZ	Capping actin protein of muscle Z-line
CAPZA1	Capping actin protein of muscle Z-line alpha subunit 1
EMT	Epithelial-mesenchymal transition
F-actin	Actin filament
HCC	Hepatocellular carcinoma

HIF-1α	hypoxia inducible factor-1α
IB	Immunoblot
IP	Immunoprecipitation
MD	Moderately differentiated
MRI	Magnetic resonance image
PD	Poorly differentiated
PIP2	Phosphatidylinositol (4,5) bisphosphate
qPCR	Quantitative PCR
ROCK	Rho-associated protein kinase
siRNA	Small interfering RNA
WD	Well differentiated; Pt: patient

Appendix A. Supplementary data

Supplementary data to this article can be found online at https://doi.org/10.1016/j.canlet.2019.01.042.

References

[1] L.A. Torre, F. Bray, R.L. Siegel, J. Ferlay, J. Lortet-Tieulent, A. Jemal, Global cancer statistics, 2012, Ca - Cancer J. Clin. 65 (2015) 87–108.
[2] G.B. Goh, P.E. Chang, C.K. Tan, Changing epidemiology of hepatocellular carcinoma in Asia, Best Pract. Res. Clin. Gastroenterol. 29 (2015) 919–928.
[3] J.M. Llovet, V. Hernandez-Gea, Hepatocellular carcinoma: reasons for phase III failure and novel perspectives on trial design, Clin. Cancer Res. 20 (2014) 2072–2079.
[4] G. Qin, M. Luo, J. Chen, Y. Dang, G. Chen, L. Li, et al., Reciprocal activation between MMP-8 and TGF-beta1 stimulates EMT and malignant progression of hepatocellular carcinoma, Cancer Lett. 374 (2016) 85–95.
[5] M. Iwatsuki, K. Mimori, T. Yokobori, H. Ishi, T. Beppu, S. Nakamori, et al., Epithelial-mesenchymal transition in cancer development and its clinical significance, Cancer Sci. 101 (2010) 293–299.
[6] D.J. McGrail, R. Mezencev, Q.M. Kieu, J.F. McDonald, M.R. Dawson, SNAIL-induced epithelial-to-mesenchymal transition produces concerted biophysical changes from altered cytoskeletal gene expression, FASEB J. 29 (2015) 1280–1289.
[7] M. Yilmaz, G. Christofori, EMT, the cytoskeleton, and cancer cell invasion, Cancer Metastasis Rev. 28 (2009) 15–33.
[8] A.E. Dart, P.R. Gordon-Weeks, The role of drebrin in cancer cell invasion, Adv. Exp. Med. Biol. 1006 (2017) 375–389.
[9] J.M. Peng, R. Bera, C.Y. Chiou, M.C. Yu, T.C. Chen, C.W. Chen, et al., Actin cytoskeleton remodeling drives epithelial-mesenchymal transition for hepatoma invasion and metastasis in mice, Hepatology 67 (2018) 2226–2243.
[10] F. Cheng, Y. Shen, P. Mohanasundaram, M. Lindstrom, J. Ivaska, T. Ny, et al., Vimentin coordinates fibroblast proliferation and keratinocyte differentiation in wound healing via TGF-beta-Slug signaling, Proc. Natl. Acad. Sci. U. S. A. 113 (2016) E4320–E4327.
[11] D. Huang, L. Cao, S. Zheng, CAPZA1 modulates EMT by regulating actin cytoskeleton remodeling in hepatocellular carcinoma, J. Exp. Clin. Canc. Res. 36 (2017) 13.
[12] J.M. Brown, W.R. Wilson, Exploiting tumour hypoxia in cancer treatment, Nat. Rev. Canc. 4 (2004) 437–447.
[13] A. Maeda, Y. Chen, J. Bu, H. Mujcic, B.G. Wouters, R.S. DaCosta, In vivo imaging reveals significant tumor vascular dysfunction and increased tumor hypoxia-inducible factor-1alpha expression induced by high single-dose irradiation in a pancreatic tumor model, Int. J. Radiat. Oncol. Biol. Phys. 97 (2017) 184–194.
[14] R. Huber, B. Meier, A. Otsuka, G. Fenini, T. Satoh, S. Gehrke, et al., Tumour hypoxia promotes melanoma growth and metastasis via High Mobility Group Box-1 and M2-like macrophages, Sci. Rep. 6 (2016) 29914.
[15] S. Terry, S. Buart, T.Z. Tan, G. Gros, M.Z. Noman, J.B. Lorens, et al., Acquisition of tumor cell phenotypic diversity along the EMT spectrum under hypoxic pressure: consequences on susceptibility to cell-mediated cytotoxicity, OncoImmunology 6 (2017) e1271858.
[16] X.X. Xiong, X.Y. Qiu, D.X. Hu, X.Q. Chen, Advances in hypoxia-mediated mechanisms in hepatocellular carcinoma, Mol. Pharmacol. 92 (2017) 246–255.
[17] L. Zhang, G. Huang, X. Li, Y. Zhang, Y. Jiang, J. Shen, et al., Hypoxia induces epithelial-mesenchymal transition via activation of SNAI1 by hypoxia-inducible factor -1alpha in hepatocellular carcinoma, BMC Canc. 13 (2013) 108.
[18] W.H. Fan, F.J. Du, X.J. Liu, N. Chen, Knockdown of FRAT1 inhibits hypoxia-induced epithelial-to-mesenchymal transition via suppression of the Wnt/beta-catenin pathway in hepatocellular carcinoma cells, Oncol. Rep. 36 (2016) 2999–3004.
[19] Q. Wen, P.A. Janmey, Polymer physics of the cytoskeleton, Curr. Opin. Solid State Mater. Sci. 15 (2011) 177–182.
[20] E. Jacinto, R. Loewith, A. Schmidt, S. Lin, M.A. Ruegg, A. Hall, et al., Mammalian TOR complex 2 controls the actin cytoskeleton and is rapamycin insensitive, Nat. Cell Biol. 6 (2004) 1122–1128.
[21] M.W. Kilimann, G. Isenberg, Actin filament capping protein from bovine brain, EMBO J. 1 (1982) 889–894.
[22] B.C. Suh, B. Hille, PIP2 is a necessary cofactor for ion channel function: how and why? Annu. Rev. Biophys. 37 (2008) 175–195.
[23] N. Thapa, R.A. Anderson, PIP2 signaling, an integrator of cell polarity and vesicle trafficking in directionally migrating cells, Cell Adhes. Migrat. 6 (2012) 409–412.
[24] M. Yamamoto, D.H. Hilgemann, S. Feng, H. Bito, H. Ishihara, Y. Shibasaki, et al., Phosphatidylinositol 4,5-bisphosphate induces actin stress-fiber formation and inhibits membrane ruffling in CV1 cells, J. Cell Biol. 152 (2001) 867–876.
[25] Z. Liu, K. Tu, Y. Wang, B. Yao, Q. Li, L. Wang, et al., Hypoxia accelerates aggressiveness of hepatocellular carcinoma cells involving oxidative stress, epithelial-mesenchymal transition and non-canonical hedgehog signaling, Cell. Physiol. Biochem. 44 (2017) 1856–1868.
[26] S. Tohme, H.O. Yazdani, Y. Liu, P. Loughran, D.J. van der Windt, H. Huang, et al., Hypoxia mediates mitochondrial biogenesis in hepatocellular carcinoma to promote tumor growth through HMGB1 and TLR9 interaction, Hepatology 66 (2017) 182–197.
[27] X. Chen, S. Zhang, Z. Wang, F. Wang, X. Cao, Q. Wu, et al., Supervillin promotes epithelial-mesenchymal transition and metastasis of hepatocellular carcinoma in hypoxia via activation of the RhoA/ROCK-ERK/p38 pathway, J. Exp. Clin. Canc. Res. 37 (2018) 128.
[28] T. Nishikawa, T. Takahashi, M. Nakamori, Y. Yamazaki, T. Kurashige, Y. Nagano, et al., Phosphatidylinositol-4,5-bisphosphate is enriched in granulovacuolar degeneration bodies and neurofibrillary tangles, Neuropathol. Appl. Neurobiol. 40 (2014) 489–501.
[29] A.F. Chambers, A.C. Groom, I.C. MacDonald, Dissemination and growth of cancer cells in metastatic sites, Nat. Rev. Canc. 2 (2002) 563–572.
[30] E. Sahai, Illuminating the metastatic process, Nat. Rev. Canc. 7 (2007) 737–749.
[31] K. Wolf, S. Alexander, V. Schacht, L.M. Coussens, U.H. von Andrian, J. van Rheenen, et al., Collagen-based cell migration models in vitro and in vivo, Semin. Cell Dev. Biol. 20 (2009) 931–941.
[32] S.L. Lee, P. Rouhi, J.L. Dahl, D. Zhang, H. Ji, G. Hauptmann, et al., Hypoxia-induced pathological angiogenesis mediates tumor cell dissemination, invasion, and metastasis in a zebrafish tumor model, Proc. Natl. Acad. Sci. U. S. A. 106 (2009) 19485–19490.
[33] J. Zhou, K. Li, Y. Gu, B. Feng, G. Ren, L. Zhang, et al., Transcriptional up-regulation of RhoE by hypoxia-inducible factor (HIF)-1 promotes epithelial to mesenchymal transition of gastric cancer cells during hypoxia, Biochem. Biophys. Res. Commun. 415 (2011) 348–354.
[34] A. Fujimura, H. Michiue, Y. Cheng, A. Uneda, Y. Tani, T. Nishiki, et al., Cyclin G2 promotes hypoxia-driven local invasion of glioblastoma by orchestrating cytoskeletal dynamics, Neoplasia 15 (2013) 1272–1281.
[35] M. Yilmaz, G. Christofori, EMT, the cytoskeleton, and cancer cell invasion, Cancer Metastasis Rev. 28 (2009) 15–33.
[36] A. Yamashita, K. Maeda, Y. Maeda, Crystal structure of CapZ: structural basis for actin filament barbed end capping, EMBO J. 22 (2003) 1529–1538.
[37] K. Zhang, D. Wang, J. Song, Cortactin is involved in transforming growth factor-beta1-induced epithelial-mesenchymal transition in AML-12 cells, Acta Biochim. Biophys. Sin. (Shanghai) 41 (2009) 839–845.
[38] J.J. Liu, J.Y. Liu, J. Chen, Y.X. Wu, P. Yan, C.D. Ji, et al., Scinderin promotes the invasion and metastasis of gastric cancer cells and predicts the outcome of patients, Cancer Lett. 376 (2016) 110–117.
[39] B.C. Suh, B. Hille, PIP2 is a necessary cofactor for ion channel function: how and why? Annu. Rev. Biophys. 37 (2008) 175–195.
[40] J.A. Pitcher, Z.L. Fredericks, W.C. Stone, R.T. Premont, R.H. Stoffel, W.J. Koch, et al., Phosphatidylinositol 4,5-bisphosphate (PIP2)-enhanced G protein-coupled receptor kinase (GRK) activity. Location, structure, and regulation of the PIP2 binding site distinguishes the GRK subfamilies, J. Biol. Chem. 271 (1996) 24907–24913.
[41] N. Thapa, R.A. Anderson, PIP2 signaling, an integrator of cell polarity and vesicle trafficking in directionally migrating cells, Cell Adhes. Migrat. 6 (2012) 409–412.
[42] D. Szatmari, B. Xue, B. Kannan, L.D. Burtnick, B. Bugyi, M. Nyitrai, et al., ATP competes with PIP2 for binding to gelsolin, PLoS One 13 (2018) e0201826.
[43] T.J. Hartman, J.L. Martin, R.J. Solaro, A.M. Samarel, B. Russell, CapZ dynamics are altered by endothelin-1 and phenylephrine via PIP2- and PKC-dependent mechanisms, Am. J. Physiol. Cell Physiol. 296 (2009) C1034–C1039.
[44] J. Li, B. Russell, Phosphatidylinositol 4,5-bisphosphate regulates CapZbeta1 and actin dynamics in response to mechanical strain, Am. J. Physiol. Heart Circ. Physiol. 305 (2013) H1614–H1623.
[45] B. Xu, G. Song, Y. Ju, X. Li, Y. Song, S. Watanabe, RhoA/ROCK, cytoskeletal dynamics, and focal adhesion kinase are required for mechanical stretch-induced tenogenic differentiation of human mesenchymal stem cells, J. Cell. Physiol. 227 (2012) 2722–2729.
[46] D.M. Gilkes, L. Xiang, S.J. Lee, P. Chaturvedi, M.E. Hubbi, D. Wirtz, et al., Hypoxia-inducible factors mediate coordinated RhoA-ROCK1 expression and signaling in breast cancer cells, Proc. Natl. Acad. Sci. U. S. A. 111 (2014) E384–E393.